THE EUROPEAN PHYSICAL JOURNAL B

Regular Article

Temporal condensation and dynamic λ-transition within the complex network: an application to real-life market evolution

Mateusz Wiliński[1], Bartłomiej Szewczak[1], Tomasz Gubiec[1], Ryszard Kutner[1,a], and Zbigniew R. Struzik[2,3,4]

[1] Faculty of Physics, University of Warsaw, Pasteura 5, 02-093 Warsaw, Poland
[2] RIKEN Brain Science Institute, 2-1 Hirosawa, 351-0198 Wako-shi, Japan
[3] Graduate School of Education, The University of Tokyo, 7-3-1 Hongo, Bunkyo-ku, 113-0033 Tokyo, Japan
[4] Institute of Theoretical Physics and Astrophysics, The University of Gdańsk, Wita Stwosza 57, 80-952 Gdańsk, Poland

Abstract. We fill a void in merging empirical and phenomenological characterisation of the dynamical phase transitions in complex networks by identifying and thoroughly characterising a triple sequence of such transitions on a real-life financial market. We extract and interpret the empirical, numerical, and analytical evidences for the existence of these dynamical phase transitions, by considering the medium size Frankfurt stock exchange (FSE), as a typical example of a financial market. By using the canonical object for the graph theory, i.e. the minimal spanning tree (MST) network, we observe: (i) the (initial) dynamical phase transition from equilibrium to non-equilibrium *nucleation phase* of the MST network, occurring at some critical time. Coalescence of edges on the FSE's transient leader (defined by its largest degree) is observed within the nucleation phase; (ii) subsequent acceleration of the process of nucleation and the emergence of the *condensation phase* (the second dynamical phase transition), forming a *logarithmically diverging* temporal λ-peak of the leader's degree at the second critical time; (iii) the third dynamical *fragmentation* phase transition (after passing the second critical time), where the λ-peak *logarithmically relaxes* over three quarters of the year, resulting in a few loosely connected sub-graphs. This λ-peak (comparable to that of the specific heat vs. temperature forming during the equilibrium continuous phase transition from the normal fluid I ^{4}He to the superfluid II ^{4}He) is considered as a prominent result of a non-equilibrium superstar-like superhub or a dragon-king's abrupt evolution over about two and a half year of market evolution. We capture and meticulously characterise a remarkable phenomenon in which a peripheral company becomes progressively promoted to become the dragon-king strongly dominating the complex network over an exceptionally long period of time containing the crash. Detailed analysis of the complete trio of the dynamical phase transitions constituting the λ-peak allows us to derive a generic nonlinear constitutive equation of the dragon-king dynamics describing the complexity of the MST network by the corresponding inherent nonlinearity of the underlying dynamical processes.

1 Introduction

Although physicists have been intensively studying morphology and topology of complex networks [1–15] (and references therein) in order to understand the mechanisms responsible for the evolution of real-world complex systems, there are still some intriguing "white spots" left, particularly in the domain of dynamic phase transitions. These transitions are the generic interest of this work. Arguably, one of the most elusive among these, is the temporal condensation phenomenon, together with a λ-transition (or temporal λ-peak) associated with this phenomenon – which hitherto have never been observed in a real-world network [16]. By the term "temporal λ-peak" we understand here the temporal shape of a short-range order

parameter resembling the Greek letter λ[1]. In this work we identify the temporal λ-peak on the real-life market complex network and characterise its properties.

We study sophisticated dynamic properties of the minimal spanning tree (MST) network of assets' returns as it is a canonical "hard core" of the majority of empirical complex networks. Let us recall that the MST is a correlation based network where multiple connections and loops are not allowed [17–28] and the number of vertices, n, and edges, $n-1$, are fixed. For such a network, the inter-node distance is defined as $d(i,j) \propto \sqrt{1 - C(i,j)}$, for any pair of vertices. For comparison, we also use other

[a] e-mail: erka@fuw.edu.pl

---

[1] We adopt this terminology from the equilibrium λ-transition between the normal I ^{4}He and superfluid II ^{4}He components formed by the λ-peak of the heat capacity vs. temperature.

popular metrics, however, the obtained results are practically undistinguishable within the resolution considered in this work. Furthermore, we expect that other correlation based networks, such as the Threshold Networks and Hierarchical Networks, will give very similar results, if the threshold value and the number of hierarchy levels are assumed to be sufficiently realistic quantities [29] (and references therein).

In spite of the algorithmic simplicity of the MST construction[2], the dynamics of the MST network is still puzzling at microscale [24], because relocation of edges (links) during the evolution of the MST network, involves a rearrangement of the entire graph[3]. As such, this evolution is indeed a collective phenomenon [24] being the foundation of phase transitions, where only the algorithmic (rather than an analytic) recipe defines the network's single time-step transformation. Hence, the dynamics of this collective phenomenon provides a significant rationale for our decision to use the evolving MST network.

We demonstrate a diachronic [32] approach to condensation, complementary to those considered by Albert and Barabási [2] (and references therein) and Dorogovtsev et al. [5] (and references therein). That is, we focus both on the birth and death of condensation as dynamic phenomena, which occur as a result of the dynamic λ-transition, between two non-equilibrium states of a complex network. This leads to the condensate, which arises as a temporal superstar-like structure. This structure is manifested in the form of a temporal singularity[4] of the richest vertex defining the dynamic λ-peak of its degree (or the short-range order parameter), where both its sides diverge logarithmically. At this time, we believe this is the first work presenting the birth and death of a condensate, manifested through the temporal λ-peak, in a real-world stock market complex network.

We develop (by neglecting fluctuations, cf. Sect. VIII.1 in Ref. [33]) a phenomenological description, where the network rearrangement is derived from, and formally equivalent to the phenomenological "macroscopic" evolution equations, where the transition probabilities involved are verified in both semi-analytical and empirical ways. A "microscopic", qualitative explanation of the processes involved was formulated through a detailed observation and analysis of the evolution of the MST network on the properly prepared sequence of snapshot frames (i.e. a "film" prepared by us), where active nodes and edges were suitably marked to make systematic tracing possible[5].

A variety of complex network models show the phenomenon of condensation in which a finite fraction of

structural elements in the network (edges, triangles, etc.) turn out to be aggregated into an ultra compact subgraph, e.g. a superstar-like structure of edges (or leader), of a size distinctly smaller than the size of the network [5] (and references therein), yet sufficiently large to strongly dominate all other local structures present in this network. In the present paper we consider not only the long-lived structural condensation phenomenon but first of all, the temporal λ-peak of the leader's degree associated with this, which has never been discussed before.

In sum, the present paper substantially and significantly extends our recent work [35]. We foresee that our results, complementary in nature to those in reference [8] (and references therein), will provide a new impact on the modeling of dynamic structural and topological phase transitions and critical phenomena on financial markets [5,36–38].

The paper is organized as follows. In Section 2 the main goal is defined together with a systematic presentation of our empirical results, constituting a basis for the phenomenological considerations following in the subsequent section. That is, Section 3 concerns the complex critical dynamics of the richest vertex, as a reminiscence of network complexity. In Section 4 we discuss and summarize our results as well as highlight the most significant phenomenon found in the evolution of the MST network as a simple but sufficiently realistic and complex reference phenomenon.

2 Phenomenology of the MST network evolution

As a representative example of the complex network dynamics we take into account the evolution – in daily horizon[6] – of the most liquid number $n = 459$, of companies quoted on the Frankfurt Stock Exchange[7] (FSE) during the particularly significant and intriguing period of large FSE variability.

The entire time series considered begins on 2004-03-22 (Monday) and finishes on 2011-12-30 (Friday). However, since we use a scanning window of a duration of 400 trading days (which we found to be optimal), the centre of the scanning window scans a shorter range – from 2004-12-27 (Monday) to 2011-03-25 (Friday). This still covers the duration of the recent worldwide financial market crisis and crash (for details, please refer to the quotation plot of the SALZGITTER (SZG) AG-Stahl und Technologie company together with the DAX shown in Fig. 1 in [34]).

These 459 companies define the core of the FSE – hence, we can consider the total numbers of the MST vertices and edges as conserved quantities. The methodology based on these conserved quantities is different from that used in our earlier works [30,35], where the number of the

---

[2] The most popular algorithms are both the Prim and Kruskal ones [30] (and references therein) in this context, as no analytic routine is known.

[3] This defines the nonseparability feature, which makes for example the Granger causality analysis inadequate for the identification of causation between variables represented as time-series [31].

[4] Obviously truncated because of the finite size effect.

[5] To see better details of the snap-shot frames, it is necessary to enlarge them using the online version of the paper [34].

---

[6] We considered the evolution in both daily and weekly horizons in the arXiv version of the present work [34] obtaining consistent results.

[7] For comparison, the DAX contains only the 30 largest companies.

most liquid companies shows temporal fluctuations (we produced our film using this methodology). Both methodologies are used in the present work and the results obtained with them are essentially indistinguishable within the assumed resolution of the plots contained in this work.

More precisely, we only observe that the absolute minimum of the Mean Occupation Layer[8] (MOL), is now located at 2005-01-25 (Thursday) instead of two trading days later, i.e. at 2007-01-29 (Monday) which we observed before. Presumably, this small shift is due to the sensitivity of the MOL which is much greater than that of the Mean Tree Length [18,21,30,35,41,42]. The temporal behavior of the Mean Occupation Layer strongly helps to identify the temporal central (key) vertex of the complex network [43].

2.1 Dominant role of the SZG company

We exploit the MST to investigate transient behavior of a complex network during its evolution. We study this evolution beginning from the equilibrium structure of the stock market hierarchy long before the recent worldwide financial crash. In Figure 1 this is represented by the network (graph) at the moment registered as beginning of the subsequent evolution of the equilibrium structure to the one dominated by a superstar-like tree (superhub or dragon-king). This emergent superhub (the SZG company) is identified in Figure 2 by the large red central circle centered in the graph. Subsequently, after adaptation to the external conditions, this dissipative structure [44] decays whilst its validating conditions disappear.

It is worth noting how small the SZG vertex[9] (having a degree equal to 3) is on the graph shown in Figure 1. The size of the vertices in the graph are proportional to their degree. The circles of the same color, both in the graph and in the plot (placed in the upper row on its right-handside), represent the same company (their abbreviations are shown in the legend, while their corresponding full names can be easily found on the internet). The vertices which occupy the thirteen top positions of the rank almost all the time are colored, while the remaining vertices are in grey (although some of them also occasionally enter the top 13 list, but only for a very short time).

---

[8] It is particularly convenient to measure this size using the Mean Occupation Layer (MOL) introduced by Onnela et al. [39,40] for study of the S&P 500 index in the vicinity of Black Monday (October 19, 1987) and also in the vicinity of the currency crisis in January 1, 1998. In this context, MOL can play the role of a temporal short-range order parameter, sufficiently sensitive to the local structure of a complex network [30,35]. The more appropriate name would be *disorder parameter*, because the lesser is its value, the more star-like is the local structure.

[9] The vertex representing the SZG company is placed on the North-West part of the graph and marked using a red dot simply named SZG. To see this dot better, it is necessary to emphasize it in the online version of the paper. The same applies to other snap-shot frames.
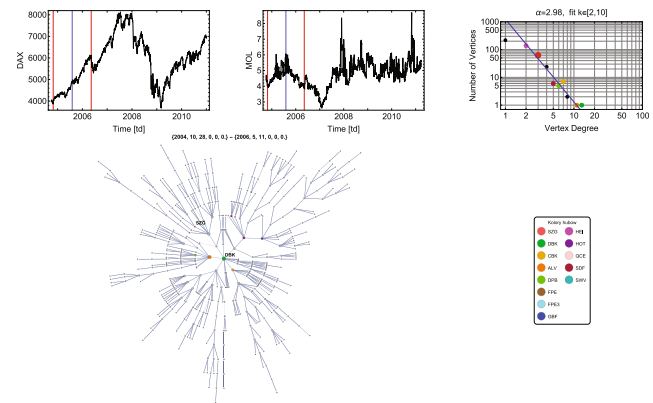

Fig. 1. Snap-shot picture of the empirical MST (graph placed in the lower row on the left-hand side of the figure) consisting of companies quoted on the FSE within the sub-period (the scanning window of 400 trading days) from 2004-10-28 (Thursday) to 2006-05-11 (Thursday) – these boundary dates are denoted by the straight vertical red lines in two plots placed in the upper row. The center of this sub-period – at 2005-08-03 (Wednesday) – is denoted by the straight vertical blue line (defining the frame of our film No. 16). The plot in log-log scale, placed in the upper row on the right-hand side of the figure, shows the fit of (unnormalized) empirical distribution of vertex degrees (small circles) by a power law (solid sloped straight line). Notably, the boundary companies (having a degree equal to 1) are coming off the power law (in all snap-shot pictures) as a result of a finite size effect. The colored circles in this plot represent not only the corresponding companies but also others of the same vertex degree. For instance, the bright green circle represents the DPB vertex (having a degree equal to 6) and four other companies having the same degree. The name abbreviations of the thirteen most significant companies (marked by the color circles – the same ones in the plot and graph) are listed in the legend (placed in the right lower corner of the figure).

Apparently, the superhub (shown in Fig. 2), decorated by the hierarchy of trees mainly placed in its first three coordination zones (or occupation layers), represents the market structure during the sub-period surrounding the crash.

Furthermore, the networks presented in Figures 1–3 have different but essentially typical modular structure.

All the snap-shot pictures obtained from our film (Figs. 1–3), were calculated using a methodology which considers a fluctuating number of the most liquid companies quoted on the FSE.

For a methodology considering a fixed number of companies, the maximal vertex degree equals 88 instead of 91 (present for the former one) and the corresponding centre of the scanning window (denoted by the vertical blue line present in the second plot in the upper row in Fig. 2) is located at $t_{\min} \equiv$ 2007-01-25 (Thursday) as the position of the absolute minimum of the MOL. This position is indistinguishable (within the assumed resolution of the plots) from date 2007-01-29 (Monday) found using the former methodology. Fortunately, this difference
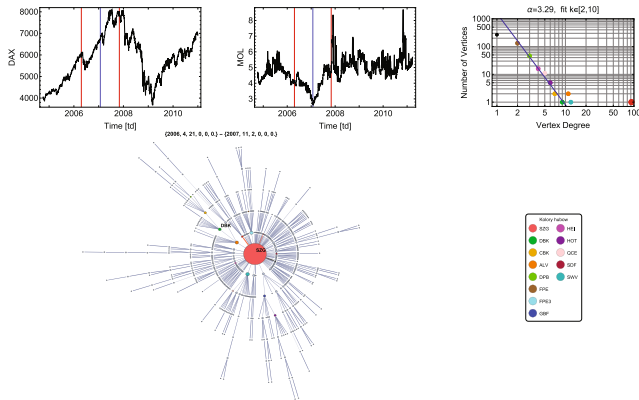
Fig. 2. Snap-shot picture of the empirical MST (graph placed in the lower row on the left-hand side of the figure) consisting of the most liquid companies quoted on the FSE within the sub-period from 2006-04-21 (Friday) to 2007-11-02 (Friday) – these boundary dates are denoted by the straight vertical red lines in both plots placed in the upper row. The center of this sub-period – at 2007-01-29 (Monday; the frame of our film No. 402) – is denoted by the straight vertical blue line. It is worth noting, how significantly the SZG company is now coming off the power law – its degree, equals 91, which is the maximal value reached by the SZG vertex during its evolution. Besides, SWV, ALV, and FPE3 companies (occupying the second and *ex aequo* the third positions in the rank, respectively) are slightly coming off this power law. These companies were already "attracted" by the SZG vertex to its first and second coordination layers (zones). Furthermore, DBK (the initial leader, when the MST network was in the "Equilibrium scale-invariant network" – see Figs. 1 and 4 for details) now occupies the fourth position in the rank and is located in the second coordination zone. In fact, all these companies are now located much more closely to the SZG vertex than earlier, i.e. during the nucleation process [45–47] (see Figs. 13 and 14 for details).

Fig. 3. Snap-shot picture of the empirical MST (graph placed in the lower row on the left-hand side of the figure) consisting of companies quoted on the FSE within the sub-period from 2006-11-27 (Monday) to 2008-06-09 (Monday) – these boundary dates are denoted by the straight vertical red lines in both plots placed in the upper row. The center of this sub-period – at 2007-09-03 (Monday; the frame of the film No. 558) – is denoted by the straight vertical blue line. Now, the strong rearrangement of the MST network is well seen, e.g. in comparison with the corresponding one presented in Figure 2, as seven vertices are coming off the power law, although, the SZG company still occupies the leading position. The colored circles in this plot represent not only the corresponding companies but also others of the same vertex degree, e.g. the orange circle represents not only ALV but simultaneously SWV (dark blue circle placed in the graph) and FPE (brown circle placed in the graph).

has no noticeable influence on any of our results. Indeed, the date $t_{\min}$ appears several times in our further considerations (cf. Figs. 4 and 15 as well as Figs. 5–7 and 9), becoming the most significant parameter of our considerations obtained directly from the empirical data (and not from a fit to the data).

The central element of the structure presented in Figure 1 is the two-node core consisting of the DBK (green circle) and ALV (orange circle) companies of degrees greater than 10. Apparently, the two largest companies the DBK (Deutsche Bank AG) and ALV (Allianz SE; the green and orange circles, respectively, placed in the centre of the graph in Fig. 1) are direct neighbors for the period under consideration (i.e. for the "Equilibrium scale-invariant network" shown in Fig. 4). This occurs when the largest companies become coupled by the strongest mutual correlations, an instance which is capable of effectively balancing (or stabilizing) the entire stock market.

The structure presented in Figure 2 is superstar-like and is centered at the SZG vertex (red circle) having a degree equal to 91, i.e. much greater than the degrees of
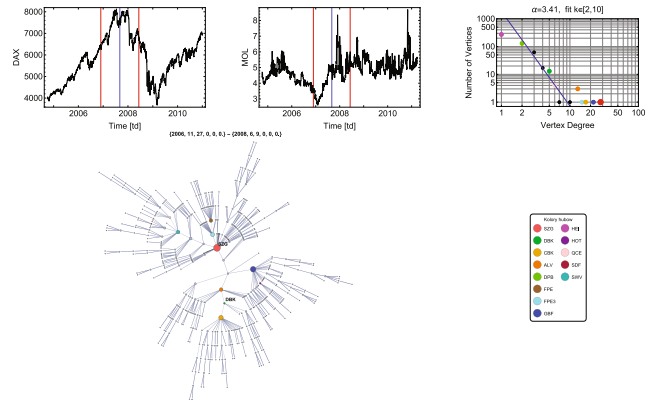
all other nodes. Later (after the crash) it takes the modular structure shown in Figure 3. This latter structure consists of two well-separated parts: the first, a single-core one centered at the SZG node (now, having a degree equal to 28) and the second, three-core structure, where separated cores are centered at GBF (navy blue circle), CBK (yellow circle), and ALV nodes of degrees greater than 15. However, this is already with only a slight SZG predominance – the vice-leader, GBF company, already has a degree equal to 22. That is, this "after-shock" MST network (concerning the sub-period of the right-hand-side of λ-peak shown in Figs. 4 and 15) is strongly decentralized consisting, at that moment, of seven well distinguished clusters centralized around the SZG, GBF, CBK, FPE3 (blue circle), ALV, SWV (dark blue circle), and FPE (brown circle) vertices.

The parameters necessary to describe the empirical data shown in Figure 4 can be separated into two different groups. To the first group belong parameters playing a significant physical role. These are: (i) the dynamical exponent z (also playing a significant role, for instance, in the scaling of autocorrelation and autoresponse functions [48]) obtained from the fit and thresholds (transition times) t_{crit} and (ii) $t_{\lambda} = t_{\min}$ made out directly from the empirical data (without any data fitting). The second group contains only the calibration parameters (unimportant for the scaling regions from a physical point of view). These parameters are as follows: (i) the mean height of the
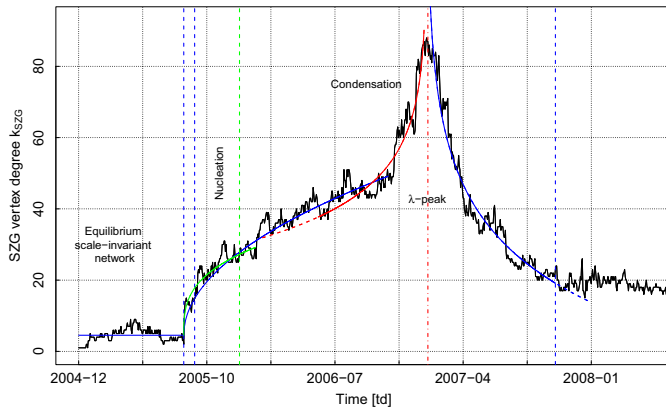
Fig. 4. The plot of the temporal SZG vertex degree, k_{SZG}, which forms, striking the eye, λ-peak. This peak is centered at $t_\lambda = t_{\min} = 544[\text{td}] \equiv 2007\text{-}01\text{-}25$ (Thursday). This centre is denoted by the dashed-dotted vertical red line. The empirical data are shown by the erratic solid black curve obtained for the daily horizon. The solid blue curve, consists of three parts: two of them placed before the maximum of the λ-peak and one after it. The height of the first horizontal blue part equals $A_0 = 4.53$ – a mean value of k_{SZG} before the first transition time or critical threshold $t_{crit} = 164[\text{td}] \equiv 2005\text{-}08\text{-}11$ (Thursday) (the location of this threshold is denoted by the first dashed vertical blue line). The long-term blue part (of the order of one year), beginning at t_{crit}, is described by a power law function $A(t - t_{crit})^{1/z} + A_0$, where the global dynamic exponent $z = 2$ and amplitude or control parameter $A = 2.50$. Apparently, this parameter distinguishes between the equilibrium scale-invariant network (for $A = 0$) and the network nucleation phase (for $A = 2.50$). However, the early stage of the nearly critical network dynamics (persisting for a period of the order of one month, that is, between two subsequent dashed vertical blue lines) is driven by the canonical Lifshitz-Slyozov dynamic exponent $z = 3$ and $A = 5.20$ (the green curve). The location of the dashed vertical green line is defined further in Figure 15, where λ-peak is better seen. The third part of the solid blue curve is defined for $0 < t - t_\lambda < \tau_R$ by the logarithmic relaxation function $-A_R \ln \left((t - t_\lambda) / \tau_R \right)$, where $A_R = 22$ and $\tau_R = 480[\text{td}]$. This function is a solution (14) of the macroscopic equation (13). The impetuously increasing solid red curve represents a logarithmic function $-A_L \ln \left((t_\lambda - t) / \tau_L \right)$, for $0 < t_\lambda - t < \tau_L$, where amplitude $A_L = 14$ and $\tau_L = 2500[\text{td}]$. The k_{SZG} short-range cross-over (of the order of one quarter) from nucleation to condensation is defined somewhere in the surroundings of 2006-07 by the overlap of solid blue and red curves, where no sharp transition is observed.

background A_0 (obtained from the empirical data utilising the fit); (ii) amplitudes A and A_J, $J = L, R$, calibrating the vertical axis, as well as (iii) the relaxation times τ_J, $J = L, R$, obtained from the fit, calibrating the horizontal axis (or time). The presence of the calibration parameters is necessary in any formula (and not only in ours) if the comparison with empirical data is required. The same remarks concern Figure 15.

It is instructive to systematically document, by using sufficiently sensitive characteristics, that the SALZGITTER (SZG) AG-Stahl und Technologie
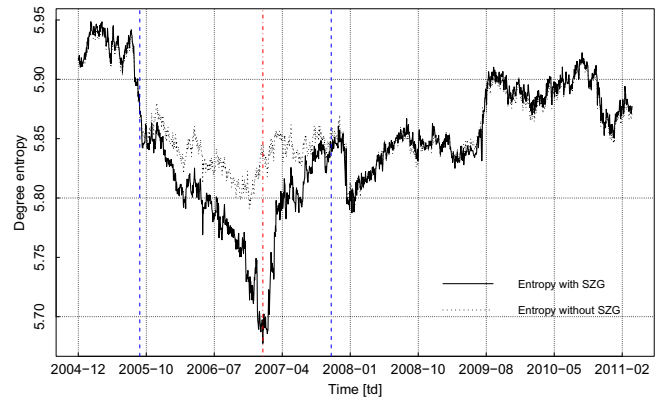

Fig. 5. Two different time-dependent entropies (based on the empirical degree distributions) derived for the MST network of the FSE, one which contains (solid curve) and one which does not contain (dotted curve) the SZG vertex (for precise entropy definition see Ref. [35]). The dashed-dotted vertical red line is located at the absolute minimum of the former entropy, i.e. at 2007-01-25 (Thursday). Apparently, no specific structure is signalized at this date by the latter entropy in contrast to the situation described by the former one. The meaning of both dashed vertical blue lines, roughly defining the range of the "funnel", was illustrated in Figure 8 and explained in its caption.

company becomes a dominant node of the Frankfurt Stock Exchange MST network during the worldwide financial and economical crisis, still persisting to date. Some initial results concerning the structural and topological phase transitions we already found on the Warsaw Stock Exchange (WSE) [30] – a complex network of 274 companies, quoted on the WSE throughout the period in question. The analogous results concerning the FSE MST were documented in our previous work [35] constituting only a starting point for the present study. In the present work we go far beyond the above mentioned results. We show, that the superhub forms a temporal structural condensate on a real-life financial market. Subsequently, we present the transition of the λ-type from this condensate to scale-invariant topology decorated by the hierarchy of local star-like hubs, representing the market structure and topology directly after the worldwide financial crash.

We study the evolution of the MST network before and after the common absolute minimum shown in Figures 5−7. We can speculate, that at this minimum the least disordered state (cf. Fig. 2) of the MST network is located, just between the preceding (cf. Fig. 1) and following (cf. Fig. 3) states of higher disorder. To be more precisely, these more disordered states are located outside the region limited by the dashed vertical blue lines, where the amplitude of the MOL variogram (taking into account the SZG vertex – denoted by the solid curve) shown in Figure 8 is distinctly higher than inside this region. Such a behaviour is typical for a random variable remaining in the surroundings of a stable fixed point for a longer time.

The significance of the central role of the SZG company within the sub-period from 2005-09-16 (Friday) to 2007-12-14 (Friday) (limited by dashed vertical blue lines
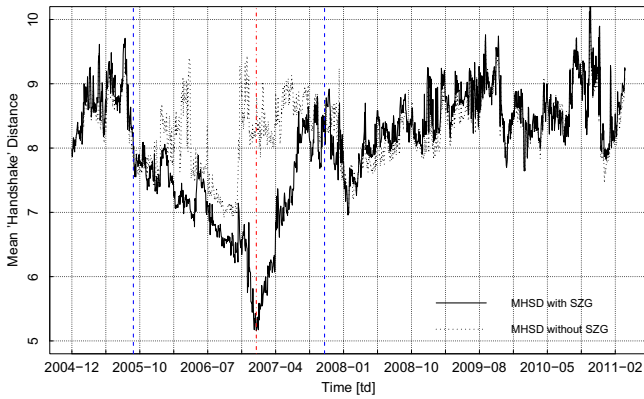
Fig. 6. Mean "Handshake" Distance (MHSD) calculated for the MST networks vs. time which contains (solid curve) and does not contain (dotted curve) the SZG vertex. This mean internode distance between a pair of vertices is measured by the mean number of edges forming a unique path connecting the pair of vertices. The absolute minimum of MHSD, placed again at 2007-01-25 (Thursday), was denoted by the dashed-dotted vertical red line. In the surroundings of this minimum, the MST network containing the SZG vertex can be considered as a compact and "small world"-like network (because then the MHSD roughly equals $\ln n$). Apparently, the MST network which does not contain the SZG vertex is much less compact. The meaning of both dashed vertical blue lines is the same as those plotted in Figure 5 and in Figures 7–9.
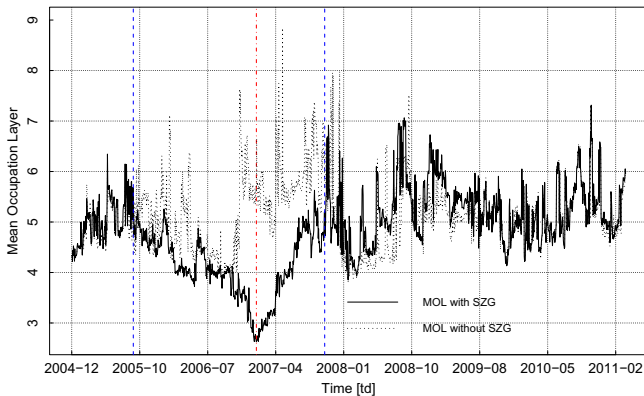

Fig. 7. Two mean occupation layers (MOLs) calculated for different MST networks: for the first MST containing the SZG vertex (solid curve) and for the second one which does not contain the SZG vertex (dotted curve). The essential difference between both various MOLs is a relatively deep absolute minimum present for the former MOL placed at 2007-01-25 (Thursday). This absolute minimum (denoted by the dashed-dotted vertical red line) and those shown in Figures 5 and 6, coincide by falling on the same trading day. Thus, the key role of the SZG vertex is extracted as the MST centre.

plotted in Figs. 5–9) is well captured by the conformity of the two temporal (simplified) betweennesses, b_{SZG} and b_2 (defined by Eq. (137) in Ref. [8]), shown in Figure 9. Apparently, within the central peak (located around 2007-01-25 as its center), the number of paths passing through the SZG vertex is about one order of magnitude larger than those passing through the vice-leader vertex, where
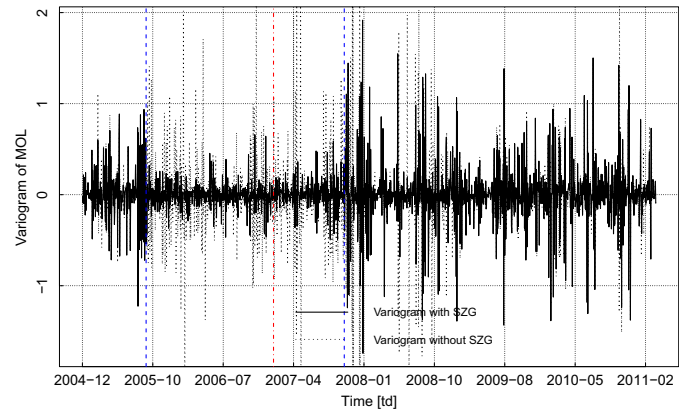

Fig. 8. Variogram of the mean occupation layer (MOL) calculated for the MST network containing the SZG vertex (solid curve) and for the MST network without the SZG vertex (dotted curve) (cf. also Fig. 7). Significant diminishing of the amplitude of the former curve (within the sub-period restricted by the dashed vertical blue lines) is well seen, in particular, in the vicinity of the MOL's absolute minimum (i.e. at 2007-01-25 (Thursday) marked by the dashed-dotted vertical red line). In other words, both dashed vertical blue lines define the time range from 2005-09-16 (Friday) to 2007-12-14 (Friday), where the amplitude of the MOL's variogram containing the SZG vertex is distinctly lower than that of the outer regions. This behavior resembles the well known one for the case of a fixed point presence. The amplitude of the solid curve is much smaller than the one of the dotted curve representing the MOL's variogram which does not contain the SZG vertex.
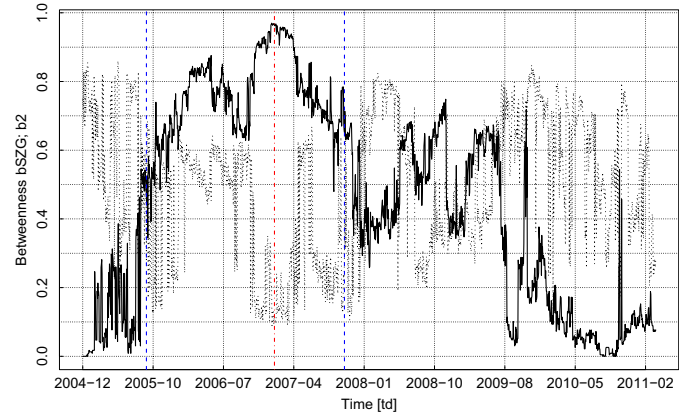

Fig. 9. Temporal betweenness [49–51] of the SZG company b_{SZG} (the solid curve) and betweenness of the vice-leader b_2 (the dashed curve). The vice-leader position is not occupied by the same company all the time. The occupation of this position varies from time to time. Remarkably, the leading position is occupied by the SZG company only when its betweenness is greater than the one of the temporal vice-leader. It takes place for the time interval limited by the dashed vertical blue lines – the same as shown in Figures 5–8. Apparently, the betweenness b_{SZG} reaches the absolute maximum at 2007-01-25 (denoted by the dashed-dotted vertical red line) that is, it reaches this maximum on the same day when the corresponding entropy, MHSD, and MOL take the absolute minimum (cf. solid curves in Figs. 5–8). Additionally, on that day the betweenness b_2 (it is then the SWV holding company) also assumes an absolute minimum.

the vice-leader vertex is defined as occupying the second position in the rank of vertex degrees. Here, it is played mainly by the SWV holding company[10] being the leader of the different 'Sector of Renewable Energy Equipment'. Indeed, the role of the SZG company is substantially greater than that of the SWV one.

In this section we showed that even the vertex which initially has a low degree can evolve towards the superhub size. Presumably, this is the result of the correlations' weakness between companies and the low cardinality of companies dominating market activity far from the crisis. Hence, the correlations of companies with the SZG became relatively more significant and they were therefore, taken into account during the preparation of the temporal MST network.

2.2 Empirical evidences for nucleation, condensation and λ-transition

This paragraph contains detailed considerations concerning the intriguing part of the MST network evolution[11], which occurs for time $t_{crit} \leq t \leq t_\lambda = t_{\min}$, where both characteristic times, t_{crit} and t_λ, were obtained directly by considering empirical characteristics of the MST network evolution – cf. Figures 4–9 and 15.

In Figure 1 the snap-shot picture presents (among others) the empirical MST scale-invariant graph concerning the sub-period ranging from 2004-10-28 (Thursday) to 2006-05-11 (Thursday), i.e. covering 400 trading days. The width of the scanning window is, indeed, fixed at this number of trading days for the entire time series duration, as it was found to be optimal (other widths equal to $300, 350, 450$, and 500 trading days were also used). This graph is characterized by a power law distribution of vertex degrees, with the exponent $\alpha = 2.98$ (see the plot in the log-log scale placed in the upper row on the right-hand side of the figure[12]). This figure clearly characterises the situation typical for the sub-period named "Equilibrium scale-invariant network" ranging from the left-hand boundary of the plot shown in Figure 4, i.e. from 2004-12-05 (Monday), to the first dashed vertical blue line located at 2005-08-11 (Thursday), that is for the MST network remaining in the equilibrium state (the properties of this state were extensively discussed in Sect. III in Ref. [34]). Remarkably, we also obtained a plot almost identical to

---

[10] SolarWorld (SWV) AG holding company is engaged in the production of the crystalline solar power technologies.
[11] Our result can be considered as a 'dynamical' example of λ-peak, inspired by the behavior of ^{4}He, which below the λ-curve is in a superfluid II ^{4}He phase, while being above it is in the normal fluid I ^{4}He phase [52]. This inspiration only has a formal character because in our study the role analogous to the temperature is played by time. That is, we deal with a dynamical phase transition and not with the equilibrium one. Considerations of the equilibrium λ-transition of ^{4}He to the superfluid phase and its hypothetical relation to the Bose-Einstein condensation can be found, e.g., in references [53,54].
[12] The temporal standard deviation, $\Delta\alpha(t)$, does not exceed 5% of the exponent $\alpha(t)$ for any time t [34].
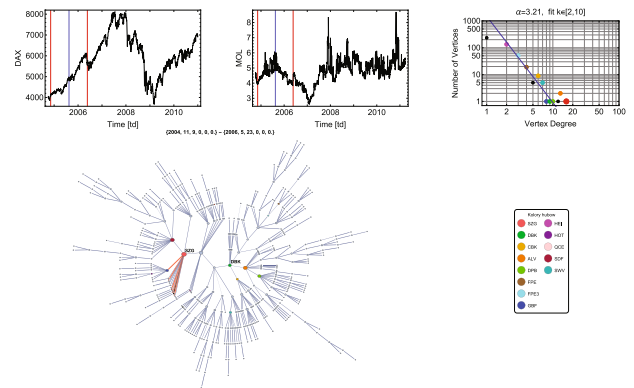

Fig. 10. Snap-shot picture of the FSE directly after the first two-day avalanche of edges attached by the SZG vertex at Monday 2005-08-15 (the frame of the film No. 24). Indeed, the red edges denote the avalanche attached in the current step to the SZG vertex, while the single black edge indicates the one which will be detached in the next time step (trading day). The enlarging of the corresponding graph presented in Figure 13 of the online version of the work [34], gives a better view. Apparently, the SZG node became a leader, as shown by the red circle in the graph and also by the corresponding red circle slightly coming off the power-law in the plot placed in the upper row on its right-hand side. The description of other elements of this Figure is analogous to that given in Figures 1 and 2 as all of them are snap-shot pictures of the same film.

that shown in Figure 4 on the weekly horizon (for details see Fig. 12 in Ref. [34]).

Notably, the power law fit (made, in all snap-shot frames in the plot on the upper row on its right-hand-side, for $2 \leq k \leq 10$) was performed by the commonly known least-square method; the maximal likelihood fit used here gives almost the same result. However, for the logarithmic binning a single decade of k range is insufficient to perform a credible fit. Nevertheless, a few points which we obtained reproduced (for all snap-shot frames) the power laws having exponents very similar to the corresponding ones obtained by the above mentioned methods. Anyhow, the principal goal of this work is to study the evolution of the superhub and not statistical properties of other nodes (e.g., their statistics). Therefore, the power law fits can be considered only as very a rough guide.

Let us focus on the SZG company (very small red circle on the graph in Fig. 1), which is now a marginal vertex since its degree hardly equals 3 (see also the red circle located in the power law plot in the log-log scale placed in the upper row on the right-hand side of the figure), but which quickly (see Fig. 10 for details) becomes a dominating vertex of the graph for about one-and-a-half year (see the sub-periods named "Nucleation" and "Condensation" in Fig. 4). Indeed, we systematically follow the "career" of this vertex by using characteristic snap-shot pictures produced by our empirically based simulation of the MST network evolution. The simulation was constructed from pictures prepared subsequently from empirical temporal daily (and, for self-consistency, also from weekly)
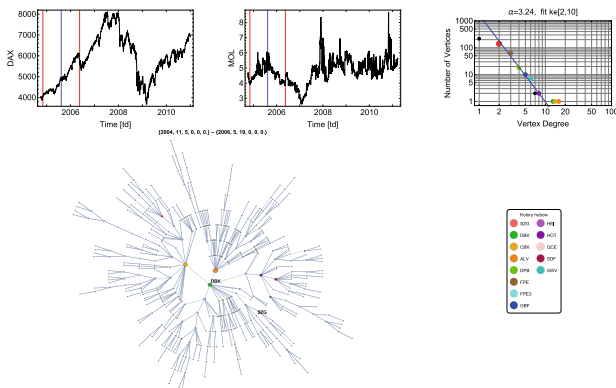
Fig. 11. Snap-shot picture of the FSE at $t_{crit} \equiv$ Thursday 2005-08-11 (the frame of the film No. 22) i.e., at the beginning of the two-day avalanche of edges attached by the SZG vertex (placed in the South-East part of the graph). Apparently, the SZG vertex is still peripheral one with a degree, which hardly equals 2 (see also the plot in the log-log scale placed in the upper row on its right-hand side) – it becomes the richest vertex only after the avalanche ends at Monday 2005-08-15 (which was visualized in Fig. 10). The largest number (10) of red unsigned dots will attach to the SZG vertex during the first day of the avalanche, i.e. during Friday 2005-08-12. The enlarging of the corresponding graph present in Figure 14 of the online version of the work [34], gives a better view.
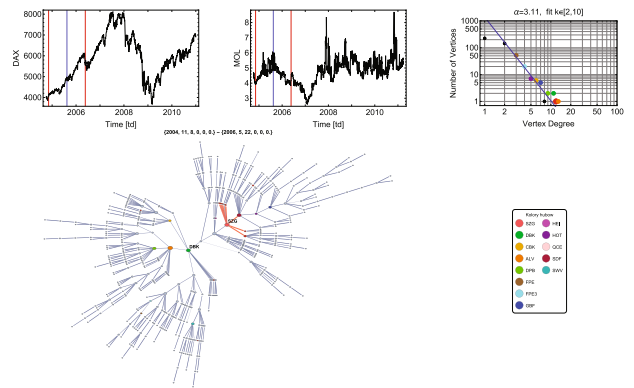
MSTs [34]. To emphasise the analysis, each snap-shot picture is supplemented with the time-dependent plots of DAX and MOL (the upper row in each figure containing the MST graph).

The leading position was reached by SZG for the first time within a very narrow region, extended in Figure 4, between the first and second dashed vertical blue lines. This position was reached in two stages. The first stage, when SZG degree abruptly increased from 2 at $t_{crit} \equiv$ Thursday 2005-08-11 (cf. Fig. 11) to 12 at Friday 2005-08-12 (cf. Fig. 12) and the second stage, when its degree again increased but now from 12 (at Friday 2005-08-12) to 16 at Monday 2005-08-15 (cf. Fig. 10). This process is sufficiently easy to see, since the edges in red denote the ones attached in the current step to the SZG vertex, while edges in black are going to be detached in the next step. Indeed, Thursday 2005-08-11 can be considered a critical time, t_{crit}, beginning the 'Nucleation' sub-period – at this moment the time translation invariance is broken. It is a beginning of the order's increase of the MST network, being an analog of the phase-ordering [48,55].

During the evolution over the "Nucleation" and "Condensation" sub-periods (see Fig. 4 for details), the SZG company still occupies the leading position, increasing its degree (up to some fluctuations) systematically. However, the manner of this increase distinctly differs for both sub-periods.

For the "Nucleation" sub-period, the degree of the SZG node only slowly, although systematically (up to some fluctuations), increases – except for the two days of abrupt increase considered above. This kind of increase is
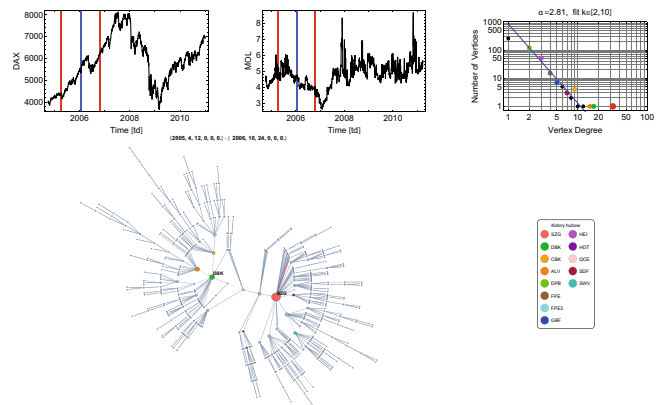

Fig. 12. Snap-shot picture of the FSE directly after the first day of the two-day avalanche of edges attached by the SZG vertex, i.e. at Friday 2005-08-12 (the frame of the film No. 23). Although the degree of the SZG node increased to 12, it still is not the richest one (it is a vice-leader at the moment). The enlarging of the corresponding graph present in Figure 15 of the online version of the work [34], gives a better view. Only after the second day of the avalanche, i.e. at Monday 2005-08-15, it already occupies the leading position (see Fig. 10 for details).

Fig. 13. Snap-shot picture concerning companies quoted on the FSE within the sub-period from 2005-04-12 to 2006-10-24 – these boundary dates are denoted, in both plots placed in the upper row, by the straight vertical red lines. The center of this sub-period – at January 16 (Monday), 2006 (the frame of the movie No. 134) – is denoted by the straight vertical blue line. Please note, how much the SZG company is now coming off the power law – here, its degree equals 32. Besides, the DBK and ALV companies (occupying the second and third positions in the rank, respectively) are only slightly coming off this power law.

determined by the structure of the MST, where very rich vertices are unfortunately located (for this sub-period) too far from the leading SZG node. This is documented by the typical situation visualized in Figure 13, where the richest nodes (DBK and ALV) are located four and five "handshakes" from the SZG node, respectively. If we notice that the SZG node mainly attaches nodes from its second and third coordination zones, it becomes clear why the SZG degree increases so slowly. The situation visualized in
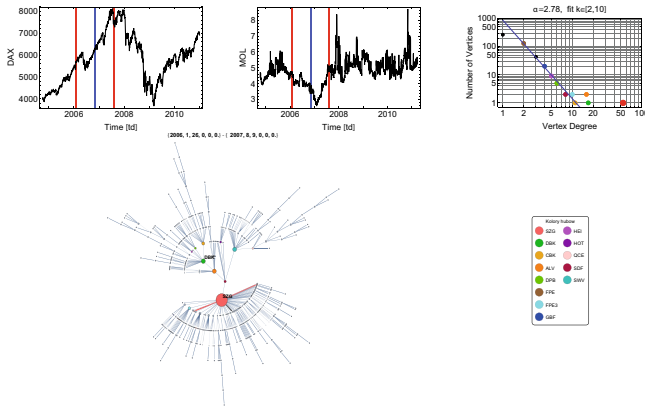
Fig. 14. Snap-shot picture concerning companies quoted on the FSE within the sub-period from 2006-01-26 to 2007-08-09 – these boundary dates are denoted, in both plots placed in the upper row, as usual by the straight vertical red lines. The center of this sub-period – at November 2 (Thursday), 2006 (the frame of the film No. 341) – is denoted (as usual) by the straight vertical blue line. Note, how much the SZG company is now coming off the power law in comparison with earlier, analogous situations (for comparison see Fig. 13) – here, its degree equals 53. This degree already quickly increases up to its maximal value equal to 91 (cf. Fig. 2). Besides, the DBK, ALV, and SWV companies (occupying the second and *ex aequo* third positions in the rank, respectively) are only slightly coming off this power law. Furthermore, DBK and ALV are now "attracted" by the SZG vertex to its second and third co-ordination layers (zones). They are now more closely located to the SZG vertex than earlier (as it is shown, for instance, in Fig. 13).

Figure 13 particularly indicates that only a single vertex (coming from the second coordination zone) will become connected to the SZG node in the next time step and that no vertex will be disconnected. This is easily seen, since the node which will be connected in the next time step is always red, while black when already disconnected in the previous step. Both here and in the entire work, the edge in red denotes the one attached to the SZG vertex in the current time step, while the edge in black is going to be detached in the next step.

In Figure 14 we already present the situation characteristic for the "Condensation" sub-period. Apparently, the four richest nodes (at the moment DBK, ALV, SWV, CBK) are located in the second and third coordination zones of the SZG. This effect of the node "attraction" by the leader is well visible in the vicinity of MOL's absolute minimum (cf. Fig. 2 and from Fig. 18 in Ref. [34]).

Furthermore, in the surroundings of the key date, i.e. 2007-01-25 (Thursday) denoted by the dashed-dotted vertical red line (the same as in Figs. 5–9), the vertices occupying the second position in the ranking are located in the first or the second coordination layer. Thus, the SZG company has at one's disposal a strongly increased number of edges. Presumably, this is the reason for the abrupt increase of the SZG degree in the vicinity of t_λ, well seen in Figures 4 and 15. For instance, during Friday 2007-01-12 (as a center of the sub-period from 2006-03-30 to
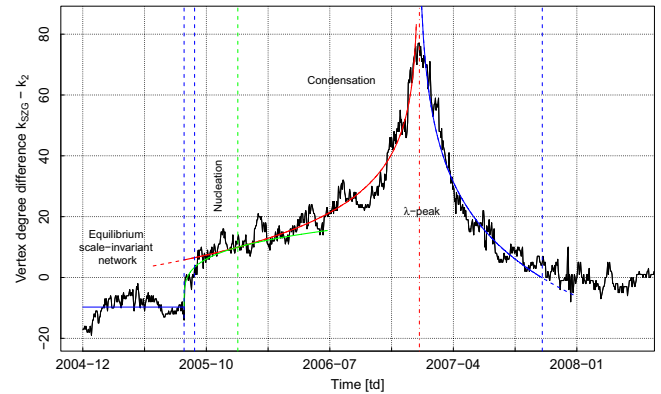

Fig. 15. The empirical, temporal vertex degree difference $k_{SZG}(t) - k_2(t)$ (erratic solid black curve obtained for the trading day horizon) vs. time t, which forms the λ-peak. The smooth well fitted red and blue diverging solid curves were obtained by using the function $-A_J^1 \ln\left(|t - t_\lambda|/\tau_J^1\right)$, $J = L, R$, for properly chosen values of calibration parameters A_J^1 and τ_J^1 for the left-hand-side ($J = L$) and right-hand-side ($J = R$) of λ-peak (cf. Tab. 2). The critical (transition) time, t_λ, is common for both sides, as is required for self-consistency. The central vertical dashed-dotted red line denotes the site of $t_\lambda = 544[td] \equiv$ 2007-01-25 (Thursday). The above mentioned diverging curves illustrate what we call the dynamic λ-transition. Additionally, the solid green curve illustrates the nucleation process defined by the expression (6). This early stage critical dynamics (driven by $z = 4$ and $A = 6.45$) was paired with the red one at the intersection defined by the dashed vertical green line located at Friday 2005-12-12 (255[td]). More refined calculations gives $3 \leq z \leq 4$. The straight horizontal blue line has a height equal to -9.73 that is, equal to the average value of all daily time-series empirical data for the period from 2004-12-01 (Wednesday) to 2005-08-12 (Friday).

2007-10-11 – the frame of the film No. 386) the number of effectively attached edges equals 13, which is a large number in comparison with other single day attachments. This is a recent large jump of k_{SZG}, placed 14 trading days before its absolute maximum, well seen in Figure 4 (a similar jump, although slightly shorter, is also seen in Fig. 15).

The above observations justify (at least partially) a canonical strategy of preferential rules frequently assumed in modeling and simulation of complex network evolutions. That is, the strong increase of the SZG degree provides an evidence for the particular form of the preferential rule valid, during approximately one year, for the richest vertex (dragon-king or core) making it increasingly richer. Furthermore, the dynamics of the entire MST network can be reduced then to the dynamics of the core that is, only to the convenient dynamics of the dragon-king (considered in Sect. 3). Hence, for instance, the structural controllability framework [56] (and references therein) of network evolution can be applied mainly to its core.

For a prolonged time (when the network passed t_λ), "repulsion" dominates "attraction" (cf. Fig. 3 for details) and the MST network decouples into several locally

centralized clusters (sectors) which leads to disintegration of the temporal condensate.

3 "Macroscopic" equation for the dragon-king non-linear dynamics

In this section we consider both the bullish and the bearish sides of the λ-peak shown in Figure 4. We focus on the dynamics of the SZG node degree, k_{SZG}, in the frame of a continuum approach. We begin with the analysis of the more complex, left-hand side of the λ-peak. In this case, the question is how its deterministic component (or the first moment) $\bar{k}_{SZG}$ increases in time. Basing ourselves on empirical observations, we assume that it increases monotonically. Effectively, this implies that there exists at least one edge attached to the SZG node at every time step, introducing a positive feedback. This edge comes from the reservoir of the remaining edges, which are not members of the first coordination zone (or the occupation layer) of the SZG node.

The description of the right-hand, relaxation side of the λ-peak follows analogously (cf. Sect. 3.3 for details).

Our approach is divided into three stages motivated by the empirical data presented in Figure 4. Within the first stage we deal with time ranging from $t_{crit} = 164$[td] $\equiv$ 2005-08-11 to the middle of October 2006 (just before the last but one k_{SZG} jump[13] shown in Fig. 4). Within the second stage we consider the time range extending from the latter date to $t_\lambda = 544$[td] $\equiv$ 2007-01-25 (the site of t_λ is denoted by the dashed-dotted vertical red line). The third stage concerns the right-hand side of λ-peak.

As we are looking for the dynamics of the first moment, $\bar{k}_{SZG}$, we disregard fluctuations (similarly as it was made in Sect. VIII.1 in Ref. [33] – see Eq. (1.7) and the equation below). That is, we are looking for an equation which relates only to the deterministic part of the corresponding (unknown) Langevin (or Fokker-Planck) equation of the process. Hence, the generic deterministic coarse-grained or "macroscopic" equation of the superstar-like evolution, formally valid for the first two stages, can be written in the clearly interpretable binomial form:

$$\frac{d\bar{k}_{SZG}\left(t'\right)}{dt} = \frac{d\bar{k}_{SZG}\left(t'\right)}{dt'} = \sum_{l=1}^{n-1-\bar{k}_{SZG}\left(t'\right)} l\, p\left(l|\bar{k}_{SZG}\left(t'\right)\right)$$
$$= \left(n-1-\bar{k}_{SZG}\left(t'\right)\right) b\left(1|\bar{k}_{SZG}\left(t'\right)\right), \quad (1)$$

---

[13] The possible inflection point can be considered as a beginning of the region of the impetuous k_{SZG} increase. However, to identify its exact location, the lower dispersion of the empirical data is required. As suggested by our present empirical data (shown in Fig. 4), we only estimate that it is located somewhere within the period from 2006-08-01 (Tuesday) to 2006-10-03 (Monday). We denoted this possible location date by the dashed vertical green line.

where $n - 1 - \bar{k}_{SZG}(t')$ is a temporal number of edges belonging to the reservoir at the time:

$$t' = \begin{cases} t - t_{crit} \ (\geq 0) & \text{for the first stage} \\ t - t_\lambda \ (< 0) & \text{for the second stage,} \end{cases} \quad (2)$$

and

$$p\left(l|\bar{k}_{SZG}(t')\right) = \binom{n-1-\bar{k}_{SZG}(t')}{l} b\left(1|\bar{k}_{SZG}(t')\right)^l$$
$$\times \left(1 - b\left(1|\bar{k}_{SZG}(t')\right)\right)^{n-1-\bar{k}_{SZG}(t')-l}. \quad (3)$$

Here, l is an effective number of edges attached to the SZG node within the time unit considered; both conditional probabilities $p(l|\bar{k}_{SZG}(t'))$ and $b(1|\bar{k}_{SZG}(t'))$ are also effective and can be interpreted as the corresponding effective rates to attach at time t' to the SZG node (which consists of $\bar{k}_{SZG}(t')$ edges) l edges and a single one, respectively. The binomial form of equation (3) states that edges are attached independently – the only dependence is that of the basic conditional probability, $b(1|\bar{k}_{SZG}(t'))$, on $\bar{k}_{SZG}(t')$.

Our goal is to derive the dependence of the basic conditional probability on $\bar{k}_{SZG}(t')$. We can expect that this probability depends both on $\bar{k}_{SZG}(t')$ and $n-1-\bar{k}_{SZG}(t')$ numbers of edges. It is because, this probability can be considered as a quotient of two other probabilities. The first joint one, $b(1,\bar{k}_{SZG}(t'))$, inversely proportional to $n - 1 - \bar{k}_{SZG}(t')$, describes an event when a single edge is randomly drawn from the reservoir. In this 'joint' case reservoir consists of $n - 1 - \bar{k}_{SZG}(t')$ edges and simultaneously the superstar-like SZG superhub consists of $\bar{k}_{SZG}(t')$ edges. The second, most significant probability $p(\bar{k}_{SZG}(t'))$ defines an event when $\bar{k}_{SZG}(t')$ edges belong to the superstar-like SZG superhub at time t'. Hence, equation (1) can be written in a form, which constitutes the basis for our further analytical considerations

$$\frac{d\bar{k}_{SZG}(t')}{dt'} \propto \frac{1}{p\left(\bar{k}_{SZG}(t')\right)}. \quad (4)$$

To complete this generic "macroscopic" equation, its right-hand-side should be given in an explicit form.

To better understand why the growth rate of the superstar-like superhub is inversely proportional to the probability $p(\bar{k}_{SZG}(t'))$, we should recognize that this probability decreases if the degree $\bar{k}_{SZG}(t')$ increases – a larger degree is less probable to occur. Hence, equation (4) simply means that the larger degree, although less probable, is a more attractive, which leads to the increase of the number of edges attached to the superstar-like superhub per time unit. This is a preferential rule concerning the superstar-like superhub, leading to the positive feedback. This type of feedback leads to the herd effect responsible for creating of the λ-peak considered in detail in Section 3.2.

In other words, equation (4) reflects the fact that the more the SZG degree increases per unit time the greater is

the SZG degree at any given time. This spells out the well-known belief that "the rich becomes richer". Nevertheless, it is difficult to become a rich node; if this happens the rate of the attaching edges also increases.

3.1 Nearly critical dynamics – the first stage

For the first stage we put forth a conjecture that the probability $p(\bar{k}_{SZG}(t'))$ has a dynamical scaling form, i.e., $p(\bar{k}_{SZG}(t')) \propto [\bar{k}_{SZG}(t') - \bar{k}_{SZG}(0)]^\gamma$, which seems to be quite a natural choice if we deal with a nearly critical dynamics. The conjecture is verified below by using the empirical data. By the term "nearly critical dynamics" we identify the dynamics which leads to a solution in the dynamical scaling form, i.e. valid within the scaling region. Hence, equation (4) takes the phenomenological form formally related to the slightly extended Allen-Cahn equation, with properly defined temporal diffusion coefficient (cf. Eqs. (3.52), (3.53) and (3.55) in Ref. [48]),

$$\frac{d\bar{k}_{SZG}(t')}{dt'} = \frac{D_0}{\left[\bar{k}_{SZG}(t') - \bar{k}_{SZG}(0)\right]^\gamma}$$
$$= \frac{D\left(\bar{k}_{SZG}(t') - \bar{k}_{SZG}(0), T\right)}{\bar{k}_{SZG}(t') - \bar{k}_{SZG}(0)}, \; A, \gamma > 0, \quad (5)$$

which has solution

$$\bar{k}_{SZG}(t') - \bar{k}_{SZG}(0) = A\, t'^{1/z}, \; z = 1 + \gamma, \quad (6)$$

where the temporal diffusion coefficient takes the formal Arrhenius form:

$$D(\bar{k}_{SZG}(t') - \bar{k}_{SZG}(0), T) = D_0 \exp\left(-E(\bar{k}_{SZG}(t') - \bar{k}_{SZG}(0))/T\right)$$

with $D_0 = \frac{A^{1+\gamma}}{1+\gamma}$, the inverted temperature $\frac{1}{T} = \gamma - 1$, and the temporal energy barrier

$$E(\bar{k}_{SZG}(t') - \bar{k}_{SZG}(0)) \stackrel{\text{def.}}{=} \ln\left(\bar{k}_{SZG}(t') - \bar{k}_{SZG}(0)\right).$$

Furthermore, the second equation in equation (6) is a particular case of equation (3.55) in [48] with $\epsilon = 1$ as the parameter. Although the diffusion coefficient is explicitly present in the right-hand-side of equation (5), the right-hand-side contains only time- and not space-dependent quantity. That is, it cannot be presented in the diffusion form as the short-range order parameter, $\bar{k}_{SZG}(t') - \bar{k}_{SZG}(0)$, does not depend on the space variable. Therefore we deal here with a non-conserved short-range order parameter, which plays a role analogous to the time-dependent linear size of the clusters in the random-site Ising model, yet different from the one considered in the present paper (cf. Sect. 3.5 in Ref. [48]).

Indeed, the solution given by equation (6) (shifted by the average height of the background $A_0 > 0$) was well fitted to empirical data, forming the "Nucleation" range in Figure 4. These fits (where the amplitude A and the dynamical exponent z were the only fitted parameters)

Table 1. Parameters characterizing left- and right-hand sides of the k_{SZG} λ-peak (calculated for trading day horizon in Sects. 3.2 and 3.3, respectively).

Side (J)	A_J	τ_J[td]	t_λ[td]
L	14	2500	544
R	22	480	544

are shown by the solid green ($z = 3$) and blue ($z = 2$) curves, respectively. It is worth to note that when $t \to t_{crit}^+$ the time derivative in the left-hand-side of equation (5) diverges. This means that the superstar-like superhub is ready to attach at t_{crit} an unlimited number of edges per unit time – its "capacity" increases unlimitedly which is the signature of criticality, characterised by the activity of almost all elements of the system. No further details concerning the MST network are needed to obtain such a good agreement between the predictions and empirical data, which verifies our conjecture. We believe this to be a result of the dynamical criticality reached by the MST network. The dynamical exponent z is, therefore, of a universal character and insensitive to microscopic details.

In our case we deal with growth of the mean "droplet" size or the SZG node's degree during the nucleation process with the dynamical exponent z, which is a slowly decreasing function of time, from the Lifshitz-Slyozov value $z = 3$ down to $z = 2$. This suggests, that we simultaneously observe some coupled competitive nucleation processes [57,58] having various rates.

The logarithmic increase of $\bar{k}_{SZG}(t')$ within the 'Condensation' time range requires a different form of the probability $p(\bar{k}_{SZG}(t'))$. Such a requirement substantially changes equation (5). Nevertheless, such an increase can be also formally reached (cf. [59]) by setting $z \to \infty$ in equation (6).

3.2 Diverging dynamics of a dragon king – the second stage

We postulate that for the "Condensation" time range, the probability that $\bar{k}_{SZG}(t')$ edges belong to the star-like SZG superhub is proportional to an exponential, i.e. $p(\bar{k}_{SZG}(t')) \propto \exp\left(-\bar{k}_{SZG}(t')/A_L\right)$, where A_L is a constant parameter, which can be considered as a typical value of $\bar{k}_{SZG}$. Hence, in the continuum limit, equation (4) takes the form

$$\frac{d\bar{k}_{SZG}(t')}{dt'} = \frac{A_L}{\tau_L} \exp\left(\bar{k}_{SZG}(t')/A_L\right), \quad (7)$$

where it is convenient to keep a proportionality constant as the ratio of both the positive parameters A_L and τ_L. The above equation describes the exponential increase of growth rate, providing the calibration of A_L and τ_L from the fit to the empirical data – their values are summarized in Table 1.

It is a straightforward procedure to find a solution of equation (7) – it takes, for $t_\lambda - t < \tau_L$, the following

logarithmic form,

$$\bar{k}_{SZG}(t') = -A_L \ln\left(\frac{t_\lambda - t}{\tau_L}\right), \qquad (8)$$

where τ_L plays the role of the characteristic time of growth. Apparently, expression (8) logarithmically diverges at the centre of λ-peak that is, when $t \to t_\lambda^-$. Indeed, this solution fits the empirical data well as shown in Figure 4 by the solid red curve. Remarkably, t_λ was independently obtained from the empirical data as a position of the local absolute maximum of the λ-peak[14] – its value is also shown in Table 1.

3.3 Constitutive equation

The right-hand side of the λ-peak can be considered by assuming (in agreement with the empirical data) that the deterministic part of this side monotonically decreases with time. We respectively modify equation (1) obtaining,

$$\frac{d\bar{k}_{SZG}(t')}{dt'} = -\sum_{l=1}^{\bar{k}_{SZG}(t')} l\, p\left(-l|\bar{k}_{SZG}(t')\right)$$
$$= -\bar{k}_{SZG}(t')b\left(-1|\bar{k}_{SZG}(t')\right), \qquad (9)$$

where we also express the conditional probability per unit time, $p(-l|\bar{k}_{SZG}(t'))$, of disconnection of l edges from the SZG superhub at time $t' = t - t_\lambda$ (> 0), by the proper binomial representation,

$$p\left(-l|\bar{k}_{SZG}(t')\right) = \binom{\bar{k}_{SZG}(t')}{l} b\left(-1|\bar{k}_{SZG}(t')\right)^l$$
$$\times \left(1 - b\left(-1|\bar{k}_{SZG}(t')\right)\right)^{\bar{k}_{SZG}(t')-l}. \qquad (10)$$

Notably, the summation in equation (9) is extended up to the $\bar{k}_{SZG}(t')$ edges, which simply means that all the edges of the SZG node can change their location in the network.

Analogously, for the left-hand side of λ-peak, to solve equation (9), the explicit dependence of the basic conditional probability per unit time, $b(-1|\bar{k}_{SZG}(t'))$, on $\bar{k}_{SZG}(t')$ is required. Again, this probability can be considered as a quotient of the other two probabilities. The first, joint probability per time unit, $b(-1, \bar{k}_{SZG}(t'))$, inversely proportional to $\bar{k}_{SZG}(t')$, describes an event when a given single edge is randomly drawn from the SZG superhub. The second probability, $p(\bar{k}_{SZG}(t'))$, was already defined in Section 3. Hence, we can set a constitutive equation, which describes both sides of the λ-peak,

$$\frac{d\bar{k}_{SZG}(t')}{dt'} \propto \frac{\text{sgn}(t')}{p(\bar{k}_{SZG}(t'))}, \qquad (11)$$

where the proportionality constant (implicitly present in this equation) is positive (as in Eq. (4)) and

$$\text{sgn}(t') = \begin{cases} 0, & \text{for } t' = t - t_{crit} \text{ and } 0 \le t \le t_{crit}^- \\ 1, & \text{for } t' = t - t_{crit} \text{ or } t' = t - t_\lambda \\ & \text{and } t_{crit}^+ \le t \le t_\lambda^- \\ -1, & \text{for } t' = t - t_\lambda \text{ and } t_\lambda^+ \le t, \end{cases} \qquad (12)$$

where $t_{crit, \lambda}^{\mp}$ means t_{crit} or t_λ reached by t from their left- or right-hand sides, respectively.

For the left-hand-side of the λ-peak, this equation reduces, obviously, to equation (4). The right-hand-side of equation (11) is separately considered for different phases: nucleation, condensation, and relaxation. Thus we derived an equation which makes it possible to describe the dynamics of the core of the complex network in its phase far from equilibrium.

In the previous paragraph the probability $p(\bar{k}_{SZG}(t'))$ was proposed in the form of an exponential. Here, we use this form with conformed A_R parameter that is, proportional to $\exp\left(-\bar{k}_{SZG}(t')/A_R\right)$. In this case, equation (11) takes the form

$$\frac{d\bar{k}_{SZG}(t')}{dt'} = -\frac{A_R}{\tau_R} \exp\left(\bar{k}_{SZG}(t')/A_R\right), \qquad (13)$$

where the amplitude A_R and the relaxation time τ_R are positive quantities, estimated from the empirical data (see Tab. 1 for details).

The interpretation of the above equation is analogous to equation (7) although, herein, we consider (due to the minus sign in its right-hand-side) the rate of disconnection of edges from the superhub SZG.

It is also a straightforward procedure to find the solution of equation (13) – it takes for $t - t_\lambda < \tau_R$ the following logarithmic form

$$\bar{k}_{SZG}(t') = -A_R \ln\left(\frac{t - t_\lambda}{\tau_R}\right). \qquad (14)$$

This solution also logarithmically diverges at the centre of λ-peak that is, at $t \to t_\lambda^+$. Indeed, this solution was fitted to the empirical data[15] and plotted in Figure 4 by the solid blue curve. Remarkably, the center t_λ of the λ-peak is common for both sides of the peak (cf. Tab. 1), which confirms the self-consistency of our approach.

From above considerations we can conclude that the complexities, present in the second equality in equation (1) and the first equality in equation (9), reduce to nonlinearities present in the corresponding equations (5), (7) and (13).

We gain a better empirical view at the λ-peak in Section 3.4 by applying a complementary, relative short-range order parameter that is, the difference $\Delta_{SZG}(t) = k_{SZG}(t) - k_2(t)$, where $k_2(t)$ is the temporal degree of a vice-leader.

---

[14] Nevertheless, for self-consistency and independent verification, we also considered t_λ as a fit parameter. We found it, together with parameters A_L and τ_L, using the fit of formula (8) to empirical data. All the parameter values were identical to those obtained above using only two fit parameters. This consistency was possible because the λ-peak is very well formed.

[15] Analogously as in Section 3.2, parameter t_λ was not a fit parameter. The values of parameters, A_R, τ_R, and t_λ were presented in Table 1.

Table 2. Parameters characterizing left- and right-hand sides of λ-peak defined by the difference $k_{SZG}(t) - k_2(t)$ (calculated vs. time for trading day horizon).

Side (J)	A_J^1	τ_J^1[td]	t_λ[td]
L	16	544	544
R	25	200	544

3.4 λ-peak and condensation within the complementary order parameter

In this section we consider, by using the complementary short-range order parameter $\Delta_{SZG}(t)$ defined above, the dynamics of the richest SZG vertex[16] – or dragon-king – in the vicinity of January 25, 2007 as its evolution there is much more distinct and intriguing than for other rich vertices.

In Figure 15 the order parameter $\Delta_{SZG}(t)$ is plotted[17] for the daily horizon. For the weekly horizon we prepared an almost identical plot (for details see Fig. 25 in Ref. [34]). The second degree difference, $k_2(t) - k_3(t)$, (where $k_3(t)$ is the temporal degree of the company occupying the third position in the rank at time t) almost vanishes within the range of the peak (cf. Fig. 6 in Ref. [35]). The predominant role of the SZG company as a dragon king is, therefore, evident. It should be emphasized that this temporal peak is also of λ type, as both of its sides are well fitted by the function $-A_J^1 \ln\left(|t - t_\lambda|/\tau_J^1\right)$, where $|t - t_\lambda| < \tau_J^1$. The values of the parameters A_J^1, τ_J^1, and t_λ for the left- ($J = L$) and right-hand ($J = R$) sides of the peak for daily horizon are shown in Table 2. The critical (transition) time (or threshold) $t_\lambda = 544$[td] $\equiv$ 2007-01-25. The existence of this dynamical λ-peak confirms our earlier observations, in particular the most significant one, i.e. the common peak location (cf. Tabs. 1 and 2) or the common centre of the peak, t_λ.

Apparently, the temporal short-range order parameter $\Delta_{SZG}(t)$ is better suited to study the left-hand side of λ-peak than $k_{SZG}(t)$ itself. However, the latter one makes a more refined study of the nucleation process possible. Hence, we provide two complementary views on the same phenomenon, which make the analysis more versatile.

4 Concluding remarks

In spite of the perceived importance of the dynamical phase transitions on the financial markets, in particular when applied to the analysis of market crashes, a systematic empirical and phenomenological analysis of this phenomenon is still incomplete, with the reality invalidating the established views and contradicting the established facts.

By using the canonical MST network we studied, as a representative example, the dynamics of the Frankfurt

---

[16] The degree of the SZG vertex reaches its maximal value equal to $k_{SZG}^{max} = 88$ at January 25, 2007.

[17] The maximal value of the degree difference equals $\Delta_{SZG}^{max} = 77$ and is located at January 25, 2007.

Stock Exchange. The similarity of many stock exchange indices has been recently convincingly demonstrated (cf. Fig. 24 in Ref. [60]). Due to this similarity we can speculate that our results are not an exceptional case. Also, the systematic investigation of superstar-like structures and the study of their temporal dynamics with possible formation of peaks of degrees, and related dynamical phase transition phenomena appears as a realistic and promising undertaking. This might have possible implications in such significant problems as universality, network controllability, and crash precursors. Besides, it is still fascinating, in this context, how the market recoveres its activity after the crash – the initial concept in this direction was proposed in reference [61] as a kind of a spontaneous process. The evolution of complex network towards the crash and next the process of its recovery we consider as long-term (slow-mode) processes of a positive feedback kind. Furthermore, our brief analysis (outside this paper) shows that the Planar Maximally Filtered Graph (PMFG) presented in reference [62] conserves the superstar-like structure and provides its dynamics very similar to the dragon-king one presented herein.

The most innovative results of our work were provided in Figures 4 and 15, where several MST network phases forming the dynamical, structural and topological phase transitions are clearly shown. In these figures we completed the dynamical phase diagrams, where two critical times t_{crit} and t_λ were presented. Furthermore, we derived the generic constitutive equation (11) which described a multiphase dragon-king dynamics, as supplementary explicit dependences (nonlinear herein) of the probability $p(k_{SZG})$ vs. temporal k_{SZG} were applied, as required. These dependences implicitly contain the relation of the dragon-king to its surroundings (i.e. to the rest of the complex network). We found predictions of equation (11) in a good agreement with empirical data (cf. solid curves in Figs. 4 and 15).

By data exploration through visualizing the evolution of the MST network using our data-derived simulation film, we uncovered the mechanism behind the primary underlying process, leading from a marginal vertex at the beginning (SZG herein) to its final domination as a dragon-king – this dragon-king plays the role of the MST network's core over an exceptionally long period containing the recent crash. By using our constitutive equation we were able to describe the dynamical complexity of the MST network's core by the nonlinear preferential rule of the positive feedback type. In principle, such an approach makes it possible to study different kinds of well formed temporal peaks created on various financial markets by the largest node's degree. These peaks can be interpreted as the result of herding effects, both on their bullish and bearish sides. The concept of a complex network core was already considered earlier in a purely theoretical way [63]. In this paper we combined both concepts, i.e., the dragon-king dynamics and the superstar-like superhub one, with an empirical and phenomenological background.

In conclusion, we demonstrated the first evidence for the real-life dynamical condensation phenomenon with an

associated λ-transition, together with a preceding phase of nucleation growth. Further, we thoroughly investigated in empirical, simulational, and analytical ways, the complete phase diagrams for these intriguing dynamical phase transitions in real-world complex networks. We expect that our results will be inspiring for interdisciplinary physicists involved in a broad spectrum of disciplines studying emergence evoked by complexity. We hope that our work, providing a significant example of the dynamical paradigm of phase transitions and critical phenomena in a network as complex as the stock market, will inspire further development of a universal theory of dynamical phase transitions in evolving complex networks.

References

1. R. Albert, L.A. Barabási, Phys. Rev. Lett. **85**, 5234 (2000)
2. R. Albert, L.A. Barabási, Rev. Mod. Phys. **74**, 47 (2002)
3. G. Bonanno, G. Caldarelli, F. Lillo, R.N. Mantegna, Phys. Rev. E **68**, 046130 (2003)
4. I. Derényi, I. Farkas, G. Palla, T. Vicsek, Physica A **334**, 583 (2004)
5. S.N. Dorogovtsev, A.V. Goltsev, J.F.F. Mendes, Rev. Mod. Phys. **80**, 1275 (2008)
6. J. Lorenz, S. Battiston, F. Schweitzer, Eur. Phys. J. B **71**, 441 (2009)
7. T. Di Matteo, F. Pozi, T. Aste, Eur. Phys. J. B **73**, 3 (2010)
8. J. Kwapień, S. Drożdż, Phys. Rep. **515**, 115 (2012)
9. K.J. Mizigier, S.M. Wagner, J.A. Hołyst, Int. J. Prod. Econ. **135**, 14 (2012)
10. D. Helbing, Nature **497**, 51 (2013)
11. Th. Bury, J. Stat. Mech. **2013**, P11004 (2013)
12. R.N. Mantegna, J. Kértesz, New J. Phys. **13**, 025011 (2011)
13. S. Drożdż, J. Kwapień, P. Oświęcimka, R. Rak, New J. Phys. **12**, 105003 (2010)
14. P. Sieczka, J.A. Hołyst, Eur. Phys. J. B **71**, 461 (2009)
15. T. Jia, M. Pósfai, Sci. Rep. **4**, 1 (2014)
16. S.N. Dorogovtsev, *Lectures on Complex Networks* (Clarendon Press, Oxford, 2010)
17. B. Bollobás, *Modern Graph Theory* (Springer, Berlin, 1998)
18. R.N. Mantegna, Eur. Phys. J. B **11**, 193 (1999)
19. G. Bonanno, G. Calderelli, F. Lillo, S. Micciche, N. Vandewalle, R.N. Mantegna, Eur. Phys. J. B **38**, 363 (1999)
20. R.N. Mantegna, H.E. Stanley, *An Introduction to Econophysics. Correlations and Complexity in Finance* (Cambridge University Press, Cambridge, 2000)
21. G. Bonanno, F. Lillo, R.N. Mantegna, Quant. Financ. **1**, 96 (2001)
22. N. Vandewalle, F. Brisbois, X. Tordoir, Quant. Financ. **1**, 372 (2001)
23. L. Kullmann, J. Kertész, K. Kaski, Phys. Rev. E **66**, 026125 (2002)
24. G. Bonanno, G. Caldarelli, F. Lillo, R.N. Mantegna, Phys. Rev. E **68**, 046130 (2003)
25. M. Tumminello, T. Di Matteo, T. Aste, R.N. Mantegna, Eur. Phys. J. B **55**, 209 (2007)
26. M. Tumminello, C. Coronello, F. Lillo, S. Micciche, R.N. Mantegna, Int. J. Bifurc. Chaos **17**, 2319 (2007)
27. T. Ibuki, S. Suzuki, J. Inoue, in *Econophysics of Systemic Risk and Network Dynamics* (*New Economic Windows*), edited by F. Abergel, B.K. Chakrabarti, A. Chakraborti, A. Ghosh (Springer-Verlag, Milan, 2012), Chap. 15, p. 239
28. T. Ibuki, S. Higano, S. Suzuki, J. Inoue, A. Chakraborti, Statistical inference of co-movements of stocks during a finacial crisis, in *Proceed. Int. Meeting on Inference, Computation, and Spin Glasses, Sapporo, 2013*
29. A. Nobi, S.E. Maeng, G.G. Ha, J.W. Lee, `arXiv:1307.6974 [q-fin.GN]` (2013)
30. A. Sienkiewicz, T. Gubiec, R. Kutner, Z. Struzik, Acta Physica Polonica A **123**, 615 (2013)
31. G. Sugihara, R. May, H. Ye, C.-H. Hsieh, E. Deyle, M. Fogarty, S. Munch, Science **338**, 496 (2012)
32. Z. Burda, J.D. Correia, A. Krzywicki, Phys. Rev. E **64**, 046118 (2001)
33. N.G. van Kampen, *Stochastic Processes in Physics and Chemistry*, 3rd edn. (Elsevier, Amsterdam, 2007)
34. M. Wiliński, B. Szewczak, T. Gubiec, R. Kutner, Z.R. Struzik, `arXiv:1311.5753 [q-fin.ST]` (2013)
35. M. Wiliński, A. Sienkiewicz, T. Gubiec, R. Kutner, Z. Struzik, Physica A **392**, 5963 (2013)
36. D. Sornette, *Why Stock Markets Crash* (Princeton University Press, Princeton, Oxford, 2003)
37. W. Weidlich, G. Haag, *Concepts and Models of a Quantitative Sociology. The Dynamics of Interacting Populations* (Springer-Verlag, Berlin, 1983)
38. P. Bak, *How Nature Works: the Science of Self-organized Criticality* (Copernicus, New York, 1996)
39. J.-P. Onnela, A. Chakraborti, K. Kaski, J. Kertész, Eur. Phys. J. B **30**, 285 (2002)
40. J.-P. Onnela, A. Chakraborti, K. Kaski, J. Kertész, Physica A **324**, 247 (2003)
41. J.G. Brida, W.A. Risso, Exp. Syst. Appl. **37**, 3846 (2010)
42. B.M. Tabak, T.R. Serra, D.O. Cajueiro, Eur. Phys. J. B **74**, 243 (2010)
43. J. Rehmeyer, Nature News (2013), `DOI:10.1038/nature.2013.12447`
44. G. Nicolis, I. Prigogine, *Self-Organization in Nonequilibrium Systems: From Dissipative Structures to Order through Fluctuations* (J. Wiley & Sons, New York, 1977)
45. P. Kondratiuk, G. Siudem, J. Hołyst, Phys. Rev. E **85**, 066126 (2012)
46. G. Kondrat, K. Sznajd-Weron, Phys. Rev. E **77**, 021127 (2008)
47. G. Kondrat, K. Sznajd-Weron, Phys. Rev. E **79**, 011119 (2009)
48. M. Henkel, M. Pleimling, in *Non-Equilibrium Phase Transitions, Aging and Dynamical Scaling Far from Equilibrium* (Springer-Verlag, Berlin, 2010), Vol. 2
49. T. Di Matteo, F. Pozzi, T. Aste, Eur. Phys. J. B **73**, 3 (2010)
50. F. Pozzi, T. Di Matteo, T. Aste, Adv. Complex Syst. **11**, 927 (2008)
51. P. Bonacich, Am. J. Sociol. **92**, 1170 (1987)
52. R.N. Silver, in *Superfluid Helium and Neutron Scattering a New Chapter in the Condensate Saga* (Los Alamos Science, Summer, 1990), p. 159

53. K. Huang, *Statistical Mechanics* (J. Wiley & Sons, New York, 1963)
54. N. Proukakis, S. Gardiner, M. Davis, M. Szymańska, in *Quantum Gases. Finite Temperature and Non-Equilibrium Dynamics* in *Cold Atoms* (Imperial College Press, London, 2013), Vol. 1
55. D. Sornette, *Critical Phenomena in Natural Sciences. Chaos, Fractals, Selforganization and Disorder: Concepts and Tools*, Springer Series in Synergetics, 2nd edn. (Springer-Verlag, Heidelberg, 2004)
56. N.J. Cowan, E.J. Chastain, D.A. Vilhena, J.S. Freudenberg, C.T. Bergstrom, Plos One **7**, e38398 (2012)
57. D. Beysens, Y. Garrabos, C. Chabot, AIP Conf. Proc. **469**, 222 (1998)
58. I.S. Gutzow, J.W.P. Schmelzer, *The Vitreous State. Thermodynamics, Structure, Rheology, and Crystallization*, 2nd edn. (Springer-Verlag, Heidelberg, 2013)
59. M. Toda, R. Kubo, N. Saitô, *Statistical Physics I. Equilibrium Statistical Mechanics* (Springer-Verlag, Berlin, 1983)
60. D. Sornette, Int. J. Terraspace Eng. **2**, 1 (2009)
61. A. Majdandzic, B. Podobnik, S.V. Buldyrev, D.Y. Kenett, S. Havlin, Nat. Phys. **10**, 34 (2014)
62. M. Tumminello, T. Aste, T. Di Matteo, R.N. Mantegna, Proc. Natl. Acad. Sci. **102**, 10421 (2005)
63. S.N. Dorogovtsev, J.F.F. Mendes, A.M. Povolotsky, A.N. Samukhin, Phys. Rev. Lett. **95**, 195701 (2005)